

# Fast NMR relaxation, powder wettability and Hansen Solubility Parameter analyses applied to particle dispersibility

David Fairhurst<sup>a</sup>, Ravi Sharma<sup>b</sup>, Shin-ichi Takeda<sup>c</sup>, Terence Cosgrove<sup>d</sup>, Stuart W. Prescott<sup>e,\*</sup>

<sup>a</sup> Colloid Consultants, Ltd., Aiken, SC 29803, USA

<sup>b</sup> Mageleka Inc., Winter Park, FL 39104, USA

<sup>c</sup> Takeda Colloid Techno-Consulting Co., Ltd., Osaka 564-0051, Japan

<sup>d</sup> School of Chemistry, Cantock's Close, Bristol BS8 1TS, United Kingdom

<sup>e</sup> School of Chemical Engineering, UNSW, Sydney, Australia

## ARTICLE INFO

### Article history:

Received 26 June 2020

Received in revised form 31 August 2020

Accepted 1 September 2020

Available online 03 September 2020

### Keywords:

Dispersibility

NMR

Solvent selection

## ABSTRACT

The selection of appropriate solvents into which inorganic and organic sub-micron particles can be dispersed is important for product manufacturability and performance. Molecular-level interactions determine solvent suitability but are difficult to measure; existing experimental approaches require slow/expensive tests of dispersion stability. Solvent relaxation NMR measurements are shown to be a fast indicator of solvent suitability, with sensitivity to the solvent-particle intermolecular forces making it a reliable proxy for stability measurements. A structured approach to relaxation measurements with a selection of both good and poor solvents yields the Hansen Solubility Parameters (HSP) for the particle surface. Suitable solvents can be selected from a database of HSP values, and solvents can be blended to match the particle interface. The application of the approach is illustrated using a range of surface modified zinc oxide and aluminum oxide particles, with similarities and differences between the particle surfaces becoming evident through the analysis.

© 2020 Elsevier B.V. All rights reserved.

## 1. Introduction

Inorganic and organic pigments and dyes are important materials that are critical to the manufacture of many important commercial products such as paints, inks, cosmetics, pharmaceuticals, display devices, and ceramics [1–3]. In general, the composition of such products is complex. Not only do they contain a base fluid with a pigment/dye, their formulation also utilizes a variety of micro- and nano-sized additive materials. Particle dispersion is also crucial for many end-use product properties such as color, sensorial quality, polishing, film homogeneity, conductivity, therapeutic efficacy, opacity of paints and inks, as well as UV protection in cosmetics. Further, it is imperative for applications that particle dispersions are stable over the time-frame in which they are to be used. Ideally, dispersions should be evaluated over the life-cycle of a product, beginning in the design stage, through production and for the end product. Finally, the state of dispersion is an important issue for risk evaluation of fine particles and for classification of nano-enabled products [4].

The preparation of particle dispersions can be broken down into several steps [5–7]; these have been concisely summarized for the example of sunscreen formulations using oxides of zinc and titanium [8]. The initial

step is the incorporation of the dry powder into a liquid which can be water, an oil or a non-aqueous solvent. When a dry powder is first introduced to a liquid surface, liquid penetrates or wicks into the powder pack by capillary flow. Capillary flow into a porous medium such as powder packs was originally described by Lucas and Washburn [9,10] and more recently by others [11,12]. Initial wetting of the powder is controlled by a number of parameters including interstitial pore size, liquid viscosity, contact angle and interfacial energy [9,13]. However, after initial contact and penetration by the liquid into the powder, particles may still be agglomerated and the liquid may not have a sufficiently low interfacial tension to completely wet the available powder surface. Wetting agents - typically surfactant additives that reduce the solid/liquid interfacial tension - may be added at this time to facilitate wetting and subsequent de-agglomeration [7]. De-agglomeration is accomplished by application of high shear mixing such as ultra-sonication or mechanical mixing. The high shear action exposes fresh surface onto which the liquid is forced to spread. Entrapped air is also displaced by application of high energy mixing. At the end of this stage of the process, the powder is completely submerged in liquid. However, the particles may not remain separated for a long time as this depends on the prevailing balance of attractive and repulsion forces between the particles. Dispersing agents are often added to prevent re-aggregation (via coagulation or flocculation) of the dispersed particles to improve long-term stability

\* Corresponding author.

E-mail address: [s.prescott@unsw.edu.au](mailto:s.prescott@unsw.edu.au) (S.W. Prescott).

[7,14,15]; true dispersants adsorb at the solid-liquid interface to provide additional repulsive force but have minimal effect on the liquid surface tension [7]. Stability and shelf life are considered in specific ISO standards [16,17].

The relative stability of the dispersions prepared in different liquids can be determined by measuring sedimentation rates [18,19]; the more stable the system is the slower will be the rate. Both solvents and surfactants that adsorb and interact strongly with the powder surface are potentially more efficient at keeping the particles apart and dispersions so created will have longer sedimentation times. Polymeric surfactants are often used to sterically stabilize the particles, and polymeric thickeners may also be added to further slow particle flocculation/settling; both increase sedimentation time. However, in a surfactant-free system, it is desirable to identify the most efficient solvent or solvent mixture whereas in a system comprising solvent and surfactant it is desirable to identify the best combination of the components.

For the purposes of solvent selection for formulation, the formulator will frequently talk of *dispersibility*, however, there is no generally agreed definition for this term and its common usage varies widely across different fields and applications. The key phenomenon underpinning dispersibility is how a liquid wets a particle surface. Wetting depends crucially on the morphology and chemical nature of the material. Unfortunately, there are very few *reliable* measurement techniques to determine the wettability of powders. Contact angle measurements are only useful for flat surfaces. Interfacial tension measurements are applicable only to liquids.

It has been suggested that the Hansen Solubility Parameter (HSP) can be used to select the most appropriate solvents for wetting and dispersing nanoparticulate powder materials. [20–22]. The HSP methodology was originally developed to quantify the solubility of polymers in solvents (and solvent blends) using the premise of “like dissolves like”.

Hansen suggested that polymer-solvent interactions can be characterized by splitting the total cohesion energy ( $E$ ) of a liquid into three separate energies [23]: dispersion energy ( $E_D$ ), polar-dipolar energy ( $E_P$ ), and hydrogen bonding energy ( $E_H$ ) as shown in the following Eq. (1):

$$E = E_D + E_P + E_H \quad (1)$$

For comparison between large molecules and small molecules, division of  $E$  by molar volume  $V$  ( $\text{m}^3$ ) provides useful a scaling quantity called the cohesive energy density.

$$\frac{E}{V} = \frac{E_D}{V} + \frac{E_P}{V} + \frac{E_H}{V} \quad (2)$$

The total cohesive energy density ( $E/V$ ) is then defined as the solubility parameter  $\delta^2$ :

$$\delta^2 = \delta_D^2 + \delta_P^2 + \delta_H^2 \quad (3)$$

The unit for  $\delta$  is  $\text{MPa}^{1/2}$ .

In the Hansen method [23], a solvent is represented as a point in  $(\delta_D, \delta_P, \delta_H)$  space (“Hansen space”). The dispersibility of a powder in solvents with wide-ranging  $\delta_D$ ,  $\delta_P$ , and  $\delta_H$  values is evaluated. Using a selection protocol based on visual observation, solvents are then ranked as either a good solvent or a poor solvent depending on their ability to dissolve a solute (or as pertinent here, to disperse a powder). A “solubility sphere” with radius  $R_o$  for the solute, is constructed that marks the boundary between good and poor solvents; software such as HSPiP is able to assist the process [24].

In principle, the solubility sphere in Hansen space includes all good solvents and excludes poor ones. The center of the sphere has HSP coordinates that define the HSP properties of the solute [20,23–25].

In Hansen space, the strength of a specific solvent-solute interaction is reflected by two parameters: the distance in HSPs ( $R_a$ ) and the relative energy difference ( $RED$ ) between the two substances:

$$R_a^2 = 4(\delta_{D2} - \delta_{D1})^2 + (\delta_{P2} - \delta_{P1})^2 + (\delta_{H2} - \delta_{H1})^2 \quad (4)$$

$$RED = \frac{R_a}{R_o} \quad (5)$$

The smaller the HSP distance ( $R_a$ ) between the solvent and solute, the more likely the solute can be dissolved. The radius of the sphere  $R_o$  describes the maximum  $R_a$  for a solvent to be arbitrarily be ranked as good. In order to quantify this behavior, solvents with a  $RED < 1$  (within the sphere) indicates a good solvent and  $RED > 1$  (outside the sphere) indicates a poor solvent as illustrated in Fig. 1.

Additionally, it has been proposed [23,24] that solvent blends – even mixtures of individually poor solvents – having volume average HSP values similar to that for the powder surface will be most effective in wetting the material and producing high quality dispersions. This approach is somewhat analogous to using the hydrophile-lipophile balance (HLB) method to choose the most appropriate blend of surfactants in the emulsification of oil(s) [26].

Analytical centrifugation (AC) provides a quantitative approach for the HSP-based approach to solvent selection [20,25,27,28]. Measurement of relative sedimentation times (RST) by the AC technique is demonstrably faster, less error-prone and more quantitative than visual observation of sedimentation. Using RST values measured for a selection of solvents with varying HSP, the particle surface itself can be located within the 3D HSP space (using the HSPiP software). A small spherical region of that space then defines the HSP values of solvents that are suitable for the particle material being evaluated [24].

However, AC still has some practical limitations. For example, for very small nanoparticles (<30 nm), the settling time – even under high-speed centrifugation – can be very long. More critically, AC is influenced by the hydrodynamics of the particle settling and the details of the sample preparation as it is based on the application of Stokes Law [29]. AC performs best for spherical particles under laminar flow conditions, but such low Reynolds numbers are often not achievable over the time period of the experiment. AC also needs dilute dispersions of spherical particles with reasonably narrow particle size distributions

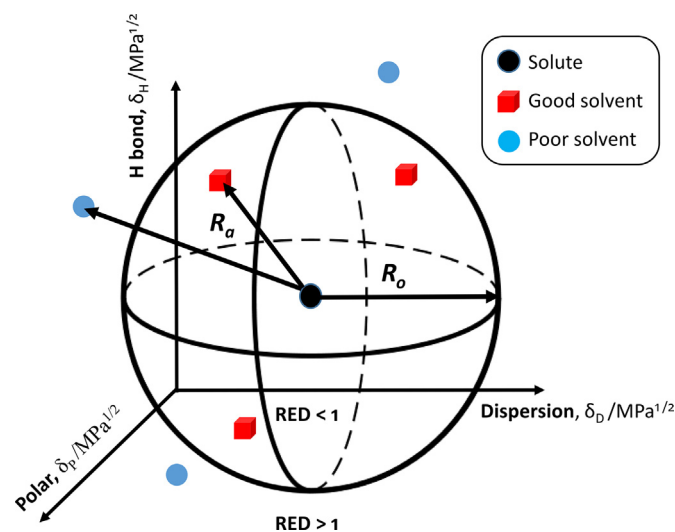


**Fig. 1.** Hansen's solubility system in the modified  $(\delta_D, \delta_P, \delta_H)$  space. The solute is located at the center of the sphere, with poor solvents for the solute (blue) outside the sphere and good solvents (red) inside the sphere. The radius of the sphere is chosen based such that a set of empirically determined solvent qualities are correctly separated by its surface. (For interpretation of the references to color in this figure legend, the reader is referred to the web version of this article.)

while many industrial materials comprise very broad particle size distributions with non-spherical particles; large particles can create turbulence as they move past the smaller particles. Solids concentrations above about 1% v/v lead to hindered settling, while industrial slurries are often prepared at high volume fraction and must therefore go through an error-prone dilution step prior to AC measurement. AC also requires knowledge of both density and viscosity of the different solvents employed in order to calculate an RST value.

As a faster and more robust alternative to AC for input into the HSP solvent selection process, we have investigated solvent relaxation NMR. The relative NMR relaxation rates of different solvents in contact with solid surfaces are indicative of a relative interaction strength (or affinity) between the specific solvent and the chosen solid surface [30,31]. Liquids exhibiting strong interactions with a particle surface have a faster NMR relaxation rate than liquids with weak interactions. Since strong interactions indicate a high affinity of solvent with the surface, we hypothesize that the single solvent, or solvent mixture, that exhibits the highest enhancement in relaxation rate would be the most suitable fluid to use for the initial wetting/dispersion process. Further, since the relative NMR relaxation rates may be ranked from good solvent (greatest relaxation rate enhancement) to poor solvent (smallest relaxation rate enhancement), relaxation rates may be used to determine the HSP values of a powder material, in the same manner as using RST determined from AC. The method is illustrated with measurements on zinc oxide and aluminum oxide powders.

## 2. NMR solvent relaxation

NMR solvent relaxation measurements are sensitive to the same intermolecular forces (as well as the dynamics) between solvent and surfaces with which HSP are concerned but they do not suffer from the limitations of the AC technique. NMR relaxation measurements are fast, direct and non-invasive; the size and shape of the powder material is immaterial. Importantly, from a practical perspective any industrially relevant solids concentration can be used. Further, the total amount of sample needed is typically *ca* 0.1 mL and can be as little as 250  $\mu\text{L}$ , making the measurement useful for expensive materials such as pharmaceutical agents.

The relaxation rate is a fundamental intrinsic property of solids and liquids and its measurement provides direct information about the extent and nature of any particle-liquid interface (e.g., suspensions and slurries) [30]. NMR relaxation works by measuring the extent of molecular motion as the hydrogen nuclei are subtly perturbed by local and external magnetic interactions. Liquids and solids behave differently. In liquids, the spin-spin relaxation is slow (taking of the order of seconds). In contrast, that for solids is very fast (less than 100 microseconds). Hence, the two relaxation rates can easily be distinguished.

The relaxation rate of the solvent in particulate suspensions is intermediate as a dynamic average of the surface relaxation rate and the bulk fluid relaxation rate; the actual value is a function of how the liquid interacts with the particle surface and the resulting interfacial structure created. The exchange of solvent molecules that strongly interact with a powder surface will be slower compared to a solvent that interacts poorly with the powder even though both solvents have completely wet the powder. Solvent relaxation is sensitive to both changes in surface area and changes in the interactions between the solvent molecules and the surface. In the case of the systems considered here, the correlation between the appropriateness of the solvent and the relaxation measurements works in the same direction in both cases: a solvent that disperses better will produce a dispersion with a higher total surface area (which would increase the relaxation rate) and also have stronger surface-solvent interactions (which would also increase the relaxation rate).

Importantly, relaxation NMR does not need the expensive, high-field, high resolution NMR instruments traditionally used for spectroscopy. The advent of small, powerful permanent magnets has made possible

the design of small, portable, benchtop low-field NMR spectrometers for characterization of particulate suspensions [32,33] and their development makes the measurement of physical properties of dispersions available to a much wider range of laboratories. These compact devices are particularly well-suited to contexts where fast, routine, measurements are needed, and in space-limited environments.

In a relaxation experiment, liquid molecules in a dispersion of particles undergo rapid exchange between the bound state (adsorbed to the particle surface) and a highly mobile free state. A spin relaxation rate constant,  $R_n$ , is determined from the reciprocal of spin relaxation time,  $T_n$  (i.e.  $R_n = 1/T_n$ ). Relaxation is manifest in both the transverse and longitudinal axes, with  $n = 1$  for spin-lattice relaxation ( $T_1$  method) and  $n = 2$  for spin-spin relaxation ( $T_2$  method). The most straightforward way to measure  $T_1$  is by the Inversion Recovery method [34]; however, the measurement is comparatively long compared with the  $T_2$  method. In this latter measurement, the Carr-Purcell-Meiboom-Gill (CPMG) method [35,36] is typically used. The choice of  $T_1$  or  $T_2$  is based upon sample characteristics such as suspension solids concentration and the chemical make-up of the dispersed phase.

The average rate,  $R_{n(av)}$ , is given by:

$$R_{n(av)} = \varphi_s R_s + \varphi_b R_b \quad (6)$$

where,  $R_s$  is the relaxation rate constant for the surface-bound liquid and  $R_b$  for the free (or bulk) liquid,  $\varphi_b$  is the fraction of liquid in the bulk phase and  $\varphi_s$  is the fraction of liquid at the surface.

The average relaxation value obtained by NMR is dependent upon the exact composition of the suspension (i.e., particle concentration, plus liquid plus additives, etc.). This is somewhat analogous to the zeta potential of a material where the measured value depends critically upon the exact composition of the dispersion fluid [37].

### 2.1. The relaxation number

Although the fundamental measurement is a relaxation time, a useful practical metric, in any application, is the relaxation number,  $R_{no}$ , which is a dimensionless parameter defined as:

$$R_{no} = (R_{susp} - R_{solv})/R_{solv} \quad (7)$$

where,  $R_{susp}$  and  $R_{solv}$  are the relaxation rates of the suspension and its (bulk) dispersion solvent, respectively. The relaxation number - which is, essentially, a relative relaxation rate enhancement - can be used to follow kinetic processes such as adsorption and desorption, and even competitive adsorption [30,31,38].

Re-arranging Eq. (5) gives:

$$R_{no} = [R_{susp}/R_{solv}] - 1 \quad (8)$$

Thus, solvents with strong interaction with a powder result in a larger  $R_{no}$  value for the suspension of that powder.

## 3. Materials, instrumentation and methods

### 3.1. Materials

Three different microfine grade zinc oxide powders were obtained from Dynamic Cosmetics, Inc., Bristol, PA, USA. All three materials are typically used in the formulation of sunscreens. One was a base (uncoated) material and the other two were coated versions of the same zinc oxide. One was coated with silica ( $\text{SiO}_2$ ) to change the surface chemistry but remain hydrophilic; the other was coated with a silane to render the surface hydrophobic, so that it could be readily dispersed in a non-aqueous fluid, such as the oil phase of a sunscreen emulsion. Their characteristics are summarized in the Table 1.

For each individual zinc oxide material, three separate dispersions were prepared in variety of solvents, at a solids concentration of 6% w/w.



**Table 1**  
Characteristics of the zinc oxides.

Coating	Surface	Aqueous behavior	$\zeta$ potential/mV	$Z_{avg}$ particle size/nm
None	Hydrophilic	Cationic	+39	122
SiO <sub>2</sub>	Hydrophilic	Anionic	–55	159
Silane	Hydrophobic	Non-wettable	N/A	138

For a specific material, the choice of solvents is somewhat arbitrary; however, the solvents must encompass a range of behavior characteristics from highly polar to highly non-polar and Hansen recommends that a minimum of twelve probe solvents be used in order to ensure maximum interrogation of a material and, hence, the most precise construction of the 3-D sphere [24].

The two alumina samples were obtained from the Sumitomo Chemical Company and their characteristics are summarized in Table 2. The two alumina dispersions were prepared at a solids concentration of 6.0% w/w for each individual alumina material - grade AKP-30 (99.99% as  $\alpha$ -alumina).

Between twelve and sixteen of the following solvents were used for each powder material: acetone (>99.9%), acetonitrile (99.8%), benzyl alcohol (99.8%), benzyl benzoate (>99.0%), butanol (>99%), caprolactone (97%), chloroform (>99.5%), cyclohexane (99.5%), cyclopentanone (>99%), decyl alcohol (>98%), dichloromethane (>99.8%), diacetone alcohol (>98%), dimethylformamide (99.8%), dimethyl sulfoxide (>99%), 1,4-dioxane (>99%), dodecane (>99%), ethanol (>99.5%), ethyl acetate (99.8%), ethyl lactate (>98%), ethyl oleate (98%), heptane (99%), hexane (>97%), isopropanol (>99.7%), methanol (>99.9%), methyl cellosolve (99.8%), methyl ethyl ketone (>99.0%), methylene chloride (>99.8%), *N*-methyl formamide (>99%), *N*-methyl pyrrolidone (>99.7%), propylene carbonate (99.7%), tetrahydrofuran (>99.9%), toluene (99.8%).

The solvents used to prepare dispersions of them were obtained from a variety of sources and used as received: Sigma-Aldrich, Tokyo Chemical Industry Company, and Wako Pure Chemical Corporation.

It is cautioned that the NMR relaxation time of any liquid is sensitive to both the water content and the presence of any dissolved oxygen (which is paramagnetic) [39,40]. Thus, the purity and source of a solvent is critical when making comparisons. Indeed, it has long been recognized that traces of polar impurities and, especially, water play a key role in any non-aqueous application [41–44]. Hence, this sensitivity of NMR relaxation suggests that the measurement can also be used as a fast quality control (QC) tool to fingerprint solvents for industrial applications.

### 3.2. Instrumentation

The zinc oxide dispersions were analyzed using a *Magnometer XRS*<sup>TM</sup> NMR spectrometer, operating at 12.5 MHz, from Mageleka Inc., Winter Park, FL, USA. A CPMG pulse sequence [35,36] was used to measure the spin–spin relaxation time; a 180° pulse spacing of 1000  $\mu$ s and up to 20,000 echoes were recorded with a 90° pulse length of 4.5  $\mu$ s.

The particle size of the zinc oxide dispersions was determined by dynamic light scattering (DLS) using a Zetasizer Nano Z, from Malvern Instruments, Westborough, MA, USA, using a 90° scattering angle. The zinc oxides were dispersed in distilled/de-ionized water containing a small amount of Aerosol AOT as a wetting agent and diluted appropriately for the DLS measurements. Zeta potentials were determined by

**Table 2**  
Characteristics of the aluminum oxides.

Coating	Surface	Aqueous behavior	$\zeta$ potential/mV	Mean particle size/nm
None	Hydrophilic	Cationic	+45	ca 300
Silane	Hydrophobic	Non-wettable	N/A	ca 300

electrophoretic light scattering (ELS) using the same Malvern Zetasizer Nano Z device. The two hydrophilic zinc oxides were dispersed in 10 mM KCl (aq); the hydrophobic zinc oxide was not measured.

The alumina dispersions were analyzed using an Acorn Area<sup>TM</sup> operating at 13.3 MHz and supplied by XiGo Nanotools, Inc., Bethlehem, PA, USA. A 180° pulse spacing of 1000  $\mu$ s and a 90° pulse length of 7  $\mu$ s was used for all measurements. The particle size and zeta potential were determined using an Electroacoustic Spectrometer DT-1202 from Dispersion Technology Inc. Bedford Hills, NY, USA.

### 3.3. Methods

#### 3.3.1. Determination of the relaxation number, ( $R_{no}$ )

For each suspension, typically, a series of five replicate scans were made and the data averaged to produce a single CPMG trace which was fitted with a single exponential to extract the relaxation time. This was then repeated for two additional suspension samples and then averaged to obtain the final relaxation time used in the calculation of the relaxation number ( $R_{no}$ ). In all cases, the repeatability of the raw relaxation time was very good (a coefficient of variance of <1.0%); hence the data is statistically robust and the differences seen are reliable. The pure solvents were measured five times using a single aliquot.

The HSP value for the different powder materials was determined using a modification of the Hansen method. In brief, the approach seeks to find a cluster of good solvents within the 3D HSP space; good solvents will have HSP values close to those of the particle surface while the rest of HSP space will contain poor solvents. The boundary between good and poor solvents is taken to be a sphere centered on the HSP values for the particle surface. The HSPiP software [24] automates the calculations for finding the region of good solvents (and identifying further suitable solvents) as follows:

1. Order the  $R_{no}$  values from smallest to largest for the range of solvents used.
2. Assign the three highest  $R_{no}$  values a score of 1 (for strong affinity), with the rest being scored 2 (for weak affinity).
3. Use the HSPiP software to construct an initial Hansen sphere for the boundary between the strong and weak affinity solvents.
4. Sequentially expand the number of solvents scored as a “1” until it is no longer possible to fit a spherical boundary between the strong and weak affinity solvents.
5. The center of this “best-fit sphere” is the effective HSP for the particulate material under investigation. The HSP locations of the final solvents with a score of “1” define the maximum value for the radius of the Hansen sphere.

Further analysis may be undertaken within HSPiP by looking for solvents with suitable HSP values using the database of solvents provided. Additionally, a triangular Teas diagram [45] using the percentages of the three interaction energies (dispersion,  $\delta_D$ , polar/dipolar,  $\delta_P$  and hydrogen bonding,  $\delta_H$ ) that comprise the HSP makes it easy to visualize the magnitude and composition of HSP for the different materials studied.

## 4. Results and discussion

### 4.1. Determination of HSP values for the particles

The NMR relaxation numbers measured for the hydrophilic and hydrophobic zinc oxide powders are shown in Fig. 2 from which it is seen that the relaxation numbers have a significant dynamic range across the selection of solvents and also that the magnitude of the relaxation number itself is markedly higher for the silica-coated material compared with the silane-coated material (by approximately a factor of 10). These NMR data demonstrate two points. First, the solvents clearly differ in their ability to separate and disperse the particles. Second, the solvent-surface interaction is an important determinant of dispersibility. As can be seen, the silane-coating makes the surface of

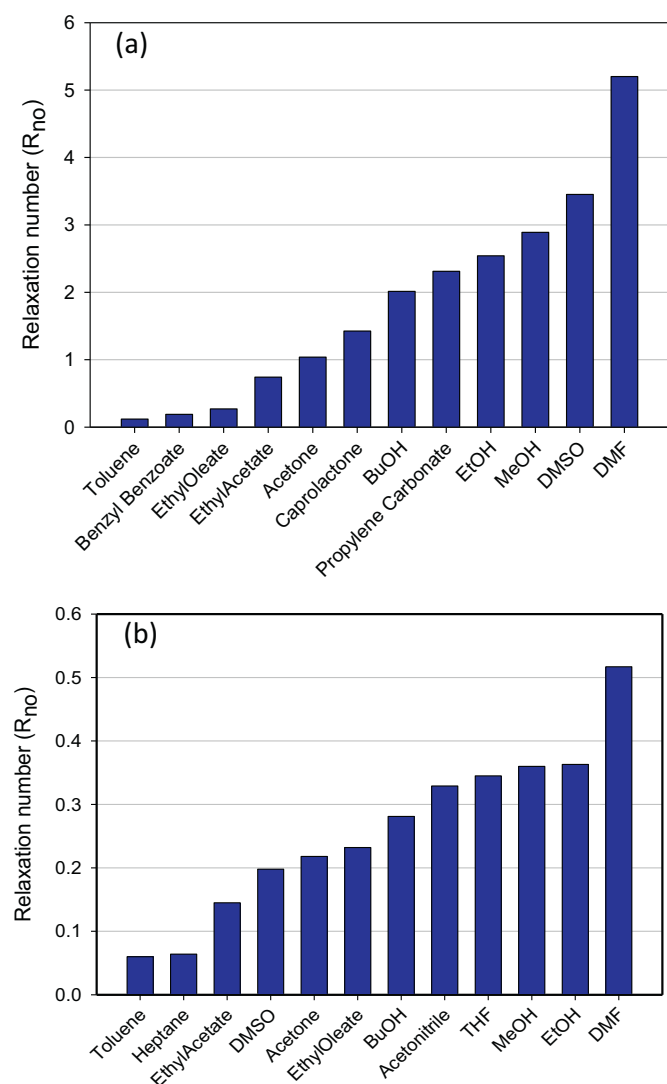


Fig. 2. Comparison of the relaxation numbers ( $R_{no}$ ) for zinc oxide powders in a variety of solvents, showing the different solvent affinity between (a) silica-coated and (b) silane-coated powders.

the zinc oxide powder so hydrophobic it is difficult to wet even with non-polar solvents. Thus, unless a wetting agent is used, it might not be possible to prepare a well-dispersed stable suspension using the non-polar solvents tested.

Following the algorithm described above, the relaxation numbers were used to derive a boundary between good and poor solvents within HSP space. Table 4 summarizes the experimental data for the silica-coated zinc oxide and Fig. 3 shows the resulting computed Hansen Sphere. As shown in Table 3, the first three of the solvents had the greatest relaxation numbers, showing the highest affinity for the particle surface and were used to construct the Hansen Sphere. The HSP for this silica-coated zinc oxide material were obtained from the sphere: Dispersion,  $\delta_D = 16.58 \text{ MPa}^{1/2}$ , Polar,  $\delta_P = 14.82 \text{ MPa}^{1/2}$  and Hydrogen Bonding,  $\delta_H = 22.11 \text{ MPa}^{1/2}$ .

Relaxation numbers for each of the powders in a variety of solvents were obtained and the same ranking/sphere fitting algorithm applied to the data in order to obtain effective HSP values for each of the particulate materials under consideration. Interestingly, it was not found possible to construct a Hansen sphere using the relaxation numbers calculated for the three zinc oxides dispersed in the solvent *N*-methyl pyrrolidone. The exact reason for this is unknown but we

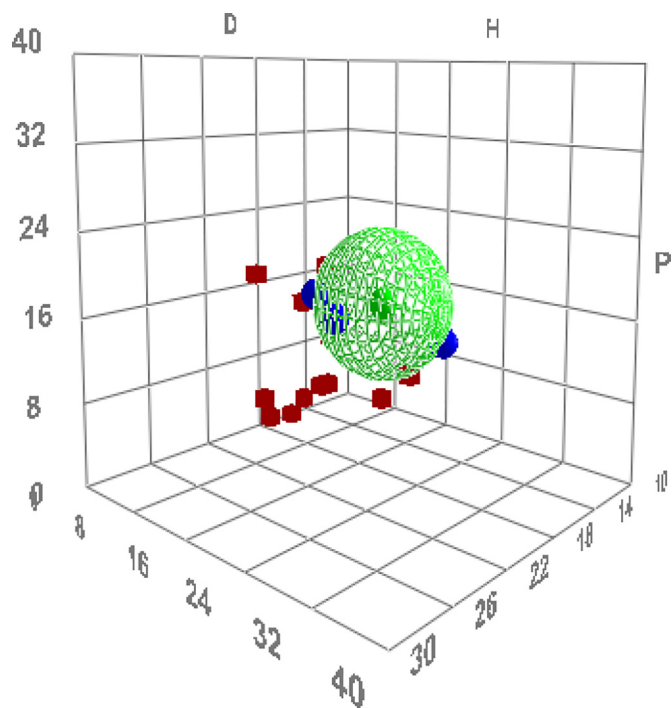


Fig. 3. The computed Hansen Sphere for the silica-coated zinc oxide based on the ranking process described above and the data in Table 4. The Hansen parameter on each axis is given in  $\text{MPa}^{1/2}$ .

speculate that it was due to the water content that adversely affected the relaxation time of the solvent. This issue is currently under further investigation.

Table 4 summarizes the data for the zinc oxides and aluminum oxides and there are differences in the combination of interaction energies between all five oxide materials. These data quantify what we intuitively know about the hydrophobized particles used here: the dispersion component ( $\delta_D$ ) is significantly higher and the hydrogen-bonding ( $\delta_H$ ) component is significantly lower for the hydrophobized powders. It can be also seen that although the NMR is only measuring a single relaxation rate for each solvent/particle pair, the assembled data permits the individual HSP values to be “triangulated” within HSP space.

#### 4.2. Application of HSP values

Once the HSP values are known for a given material, then solvent selection can be made on a rational, quantitative basis. Tables of HSP values for common solvents are readily available (such as in the HSPiP software used here); additionally, any combination of solvents whose

Table 3  
Summary of relaxation measurements for the silica-coated zinc oxide.

Solvent	Relaxation number, $R_{no}$	Takeda affinity value
Dimethyl formamide	5.20	1
Dimethyl sulfoxide	3.45	1
Methanol	2.89	1
Ethanol	2.54	2
Propylene carbonate	2.31	2
Butanol	2.01	2
Caprolactone	1.43	2
Acetone	1.04	2
Ethyl acetate	0.74	2
Ethyl oleate	0.27	2
Benzyl benzoate	0.19	2
Toluene	0.12	2

**Table 4**  
HSP parameters derived for the zinc oxides and aluminum oxide powders<sup>a</sup>.

Material	Coating	Surface	$\delta_D$ MPa <sup>1/2</sup>	$\delta_P$ MPa <sup>1/2</sup>	$\delta_H$ MPa <sup>1/2</sup>
Zinc oxide	None	Hydrophilic	15.95 (35%)	12.18 (27%)	17.64 (39%)
	SiO <sub>2</sub>	Hydrophilic	16.58 (31%)	14.82 (27%)	22.11 (42%)
	Silane	Hydrophobic	18.51 (45%)	8.97 (22%)	14.05 (34%)
Alumina	None	Hydrophilic	18.03 (36%)	12.52 (25%)	19.50 (39%)
	Silane	Hydrophobic	17.97 (58%)	6.40 (21%)	6.59 (21%)

<sup>a</sup> Values in parentheses are the percentages of each interaction energy shown in Fig. 4.

volume-average “ $\delta_D$ ”, “ $\delta_P$ ” and “ $\delta_H$ ” approximates that of the material HSP will be an effective wetting fluid. Such studies would prove useful in polymer-solvent applications [46].

The HSP values can also teach us more about the particle surfaces and the efficacy of surface modification. Using the percentages of the interaction forces shown in Table 4, TEAS plots comparing the hydrophilic and hydrophobic versions of the same particle provide useful information on their surfaces (Fig. 4). Inspection of the plots shows that the two hydrophilic zinc oxides – bare (uncoated) and silica-coated – have quite similar HSP while that for the hydrophobic, silane-coated zinc oxide is – as might be expected – different. However, there is a much larger difference between the hydrophilic, uncoated alumina and the hydrophobic, silane-coated version.

We can also see, from Fig. 4, that the HSP for the two uncoated oxides, though different, are not too disparate. While ZnO and Al<sub>2</sub>O<sub>3</sub> are clearly different chemical materials, the HSP data suggest that the interaction of solvents having strong affinity with the surface of these materials is comparable. This can be rationalized by considering that both are hydrophilic, cationic in water, and with similar zeta potentials and is likely related to the acid-base (electron acceptor-donor) properties of the surface(s) in relation to the solvent(s) [47,48].

Conversely, the type of silane coating of the oxides must be quite different, either in chemical nature or coating density. Such a marked difference affects the choice not only of the solvent used but also any other moiety – such as a surfactant, dispersant or stabilizer – that might subsequently be used in the formulation of a suspension, since it will impact the interaction (e.g., adsorption) with the surface. Thus, the HSP can be used to probe and discriminate the surface chemical nature of materials. Understanding this allows a formulator to more efficiently and better optimize the preparation of a suspension.

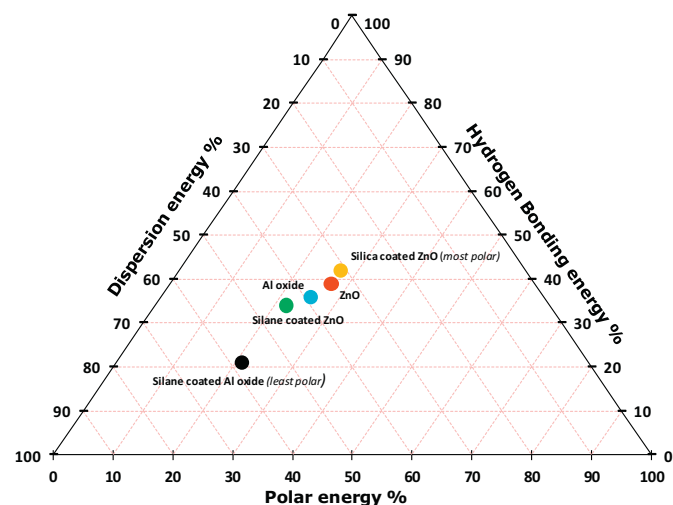


**Fig. 4.** Teas plots for all five oxide powders based on the HSP results shown in Table 4. The progression from the most polar particles (silica coated ZnO) to the most hydrophobic particles (silane coated aluminum oxide) is seen.

#### 4.3. Fast solvent screening using NMR

The above HSP analysis, a robust algorithm for solvent selection was presented that was modeled closely on established HSP sphere approaches as implemented in HSPiP. It is also possible, however, to use the NMR relaxation number as a fast screening experiment for experimental solvent selection. Throughout, the NMR relaxation number has been used as a quantitative measure of the solvent-particle interaction, and thus it is possible to use high relaxation numbers to indicate good solvents and low relaxation numbers to identify poor solvents directly, without completing the entire HSP process. We presently illustrate this with silica-coated zinc oxide dispersed in toluene, methanol and *N*-methyl pyrrolidone (NMP). The relaxation numbers were found to be 0.12, 2.89 and 7.10 respectively and on that basis we would thus predict that a longer-term stability experiment would conclude that the NMP dispersion be the most stable and the toluene dispersion the least stable.

Fig. 5 shows photographs taken of samples of silica-coated zinc oxide dispersed in these solvents as part of a stability test. Visual inspection of the dispersions immediately after preparation (Fig. 5(a)) shows that there is poor wetting of the glass vial by the toluene suspension and, initially, both the methanol and NMP suspensions look good. However, after four hours standing at room temperature it is obvious that the toluene suspension has – as might be expected – completely

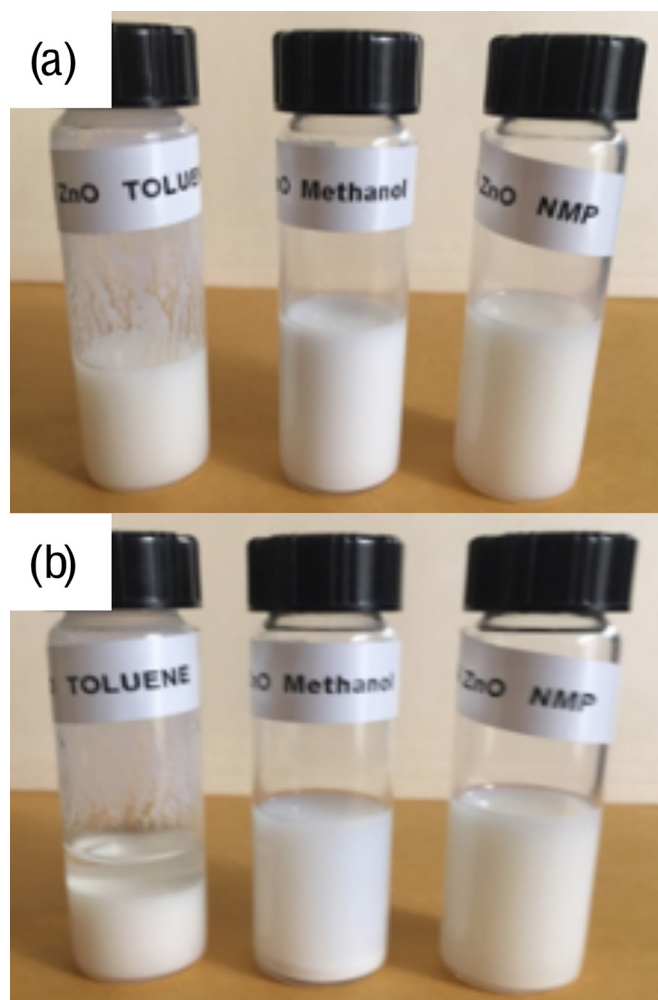


**Fig. 5.** dispersions of silica-coated zinc oxide in toluene, methanol and *N*-methyl pyrrolidone, (a) immediately after preparation, (b) four hours later. The separation and flocculation of the dispersion in toluene can be seen in the photographs and is predicted by the very low relaxation number.



separated and, indeed, appears flocculated (Fig. 5b). There is also noticeable settling in the methanol suspension but very little in the NMP suspension which still looks well dispersed.

The initial relaxation number was thus a good index of the propensity of a suspension to settle and so can provide the formulator with useful information. Since the measurement of a relaxation time takes only minutes, it can quickly provide a formulator with a measure of dispersibility well before there are any visible signs of change in concentrated suspensions.

## 5. Conclusions

In this work, we have demonstrated that NMR relaxation rates provide a way to screen solvents for suitability with various particles and, further, that they can be used to quantitatively measure solubility parameters for particulate materials.

It was observed that particles suspended in solvents identified as having weak solvent-particle interactions by NMR measurements settled relatively quickly when compared to the same particles suspended in solvents where NMR measurements had identified strong solvent-particle interactions.

These results support the hypothesis that NMR relaxation times may be used to identify solvents and surfactants for improving dispersion of sub-micron colloidal particles.

As a more sophisticated and quantitative treatment of solvent selection, the normalized relaxation rate (relaxation number) was used in rank order as the input into the HSPiP software to estimate HSP values ( $\delta_p$ ,  $\delta_D$ , and  $\delta_H$ ) for the particle surface. The NMR-determined HSP values for sample oxide materials were seen to be reasonable and follow a logical trend, while also providing additional insight into the systems. For example, we show that the two bare (uncoated) zinc oxide and aluminum oxide materials are similar (they occupy nearly identical positions in 3D Hansen space) with a large polar component. In contrast, hydrophobized zinc oxide and hydrophobized aluminum oxide each have a lower polar component compared to the bare oxide. Further, the nature of the two silane coatings is completely different; this suggests that formulating and processing of the suspensions might require different solvents and dispersing aids.

The current work suggests that NMR relaxation is a useful, rapid complimentary technique to traditional characterization methods, that relaxation measurements can help in the selection of the most suitable solvent for initial wetting and dispersing of powders, can quickly distinguish between concentrated suspensions that, initially, appear to be similar and so can provide the formulator with time-saving information.

## Declaration of Competing Interest

The authors declare that they have no known competing financial interests or personal relationships that could have appeared to influence the work reported in this paper.

The authors declare the following financial interests/personal relationships which may be considered as potential competing interests: Mageleka Inc. manufacturers bench-top NMRs.

## Acknowledgements

Prof. Steven Abbott (University of Leeds and Steven Abbott TCNF Ltd) is thanked for numerous fruitful discussions around HSP theory and the use of the HSPiP software.

## References

[1] C. Pichot, T. Delair, A. Elaïssari, Polymer colloids for biomedical and pharmaceutical applications, in: J.M. Asua (Ed.), *Polymeric Dispersions: Principles and Applications* NATO ASI Series (Series E: Applied Sciences), Springer, Dordrecht 1995, pp. 515–539.

[2] J.A. Lewis, Colloidal processing of ceramics, *J. Am. Ceram. Soc.* 83 (2000) 2341–2359.

[3] L. Bergstrom, Colloidal processing of ceramics, *Handb. Appl. Surf. Colloid Chem.* 1 (2001) 201–217.

[4] H. Rauscher, K. Rasmussen, B. Sokull-Kluttgen, Regulatory aspects of nanomaterials in the EU, *Chem-Ing-Tech* 89 (2017) 224–231.

[5] Incline, How to Disperse and Stabilize Pigments, <http://www.incline.gr/inkjet/newtech/tech/dispersion/> 2019.

[6] G.D. Parfitt, *Dispersion of Powders in Liquids*, 3rd ed. Applied Science Publishers, Amsterdam, 1969.

[7] Esaar International, What are the Differences Between Wetting Agents and Dispersants, <https://www.esaar.com/2018/10/04/what-are-the-differences-between-wetting-agents-and-dispersants/> 2018.

[8] D. Fairhurst, M.A. Mitchnick, Particulate sun blocks: general principles, in: N.J. Lowe, N.A. Shaath, M.A. P (Eds.), *Sunscreens: Development, Evaluation and Regulatory Aspects*, Marcel Dekker, New York, 1997.

[9] E.W. Washburn, The dynamics of capillary flow, *Phys. Rev.* 17 (1921) 273–283.

[10] R. Lucas, Über das Zeitgesetz des kapillaren Aufstiegs von Flüssigkeiten, *Colloid Polym. Sci.* 23 (1918) 15–22.

[11] P.M. Heertjes, W. Witvoet, Some aspects of the wetting of powders, *Powder Technol.* 3 (1969) 339–343.

[12] K.P. Haggood, J.D. Litster, S.R. Biggs, T. Howes, Drop penetration into porous powder beds, *J. Colloid Interface Sci.* 253 (2002) 353–366.

[13] R. Sharma, D.S. Ross, Kinetics of liquid penetration into periodically constricted capillaries, *J. Chem. Soc. Faraday Trans.* 87 (1991) 619–624.

[14] T. Cosgrove, *Colloid Science: Principles, Methods and Applications*, 2nd ed. Wiley, Chichester, West Sussex, 2010.

[15] S. Ross, I.D. Morrison, *Colloidal Systems and Interfaces*, Wiley, New York, 1988.

[16] ISO, ISO/TR 13097: 2013 Guidelines for the Characterization of Dispersion Stability, 2013.

[17] ISO, ISO/TR 18811: 2018: Cosmetics – Guidelines on Stability Testing of Cosmetic Products, 2018.

[18] N. Azema, Sedimentation behaviour study by three optical methods – granulometric and electrophoresis measurements, dispersion optical analyser, *Powder Technol.* 165 (2006) 133–139.

[19] S. Manjula, S.M. Kumar, A.M. Raichur, G.M. Madhu, R. Suresh, M.A.L.A. Raj, A sedimentation study to optimize the dispersion of alumina nanoparticles in water, *Cerâmica* 51 (2005) 121–127.

[20] S. Süß, T. Sobisch, W. Peukert, D. Lerche, D. Segets, Determination of Hansen parameters for particles: a standardized routine based on analytical centrifugation, *Adv. Powder Technol.* 29 (2018) 1550–1561.

[21] S. Gårdebjær, M. Andersson, J. Engström, P. Restorp, M. Persson, A. Larsson, Using Hansen solubility parameters to predict the dispersion of nano-particles in polymeric films, *Polym. Chem.* 7 (2016) 1756–1764.

[22] J.U. Wieneke, B. Kommoß, O. Gaer, I. Prykhodko, M. Ulbricht, Systematic investigation of dispersions of unmodified inorganic nanoparticles in organic solvents with focus on the Hansen solubility parameters, *Ind. Eng. Chem. Res.* 51 (2011) 327–334.

[23] C.M. Hansen, *Hansen Solubility Parameters: A User's Handbook*, 2nd ed. CRC Press, Boca Raton, 2007.

[24] Hansen, HSPiP Hansen Solubility Parameters Software, <https://www.hansen-solubility.com/HSPiP/> 2019.

[25] M. Weng, Determination of the Hansen solubility parameters with a novel optimization method, *J. Appl. Polym. Sci.* 133 (2016).

[26] P. Becher, *Principles of Emulsion Technology*, Reinhold Publishing Corporation, U.S., 1955.

[27] D. Lerche, T. Sobisch, Consolidation of concentrated dispersions of nano- and micro-particles determined by analytical centrifugation, *Powder Technol.* 174 (2007) 46–49.

[28] D. Lerche, S. Horvat, T. Sobisch, Efficient instrument based determination of the Hansen solubility parameters for talc-based pigment particles by multisample analytical centrifugation: zero to one scoring, *Dispers. Lett.* 6 (2015) 13–18.

[29] G.G. Stokes, On the effect of internal friction of fluids on the motion of pendulums, *Trans. Camb. Philos. Soc.* 9 (1851) 8–106.

[30] C.L. Cooper, T. Cosgrove, J.S. van Duijneveldt, M. Murray, S.W. Prescott, The use of solvent relaxation NMR to study colloidal suspensions, *Soft Matter* 9 (2013) 7211–7228.

[31] B. Cattoz, T. Cosgrove, M. Crossman, S.W. Prescott, Surfactant-mediated desorption of polymer from the nanoparticle interface, *Langmuir* 28 (2012) 2485–2492.

[32] D. Fairhurst, T. Cosgrove, S.W. Prescott, Relaxation NMR as a tool to study the dispersion and formulation behavior of nanostructured carbon materials, *Magn. Reson. Chem.* 54 (2016) 521–526.

[33] D. Fairhurst, S.W. Prescott, The use of nuclear magnetic resonance as an analytical tool in the characterisation of dispersion behaviour, *Spectrosc. Eur.* 23 (2011) 13–16.

[34] T.C. Farrar, E.D. Becker, *Pulse and Fourier Transform NMR; Introduction to Theory and Methods*, Academic Press, New York, 1971.

[35] H.Y. Carr, E.M. Purcell, Effects of diffusion on free precession in nuclear magnetic resonance experiments, *Phys. Rev.* 94 (1954) 630–638.

[36] S. Meiboom, D. Gill, Modified spin-Echo method for measuring nuclear relaxation times, *Rev. Sci. Instrum.* 29 (1958) 688–691.

[37] R.J. Hunter, *Zeta Potential in Colloid Science: Principles and Applications*, Academic Press, London, 1981.

[38] U.C. Rajesh, J.F. Wang, S. Prescott, T. Tsuzuki, D.S. Rawatt, RGO/ZnO nanocomposite: an efficient, sustainable, heterogeneous, amphiphilic catalyst for synthesis of 3-substituted indoles in water, *ACS Sustain. Chem. Eng.* 3 (2015) 9–18.

[39] K. Krynicki, Proton spin-lattice relaxation in pure water between 0°C and 100°C, *Physica* 32 (1966) 167–178.

- [40] M.E. Mirhej, Proton spin relaxation by paramagnetic molecular oxygen, *Can. J. Chem.* 43 (1965) 1130–1138.
- [41] D.D. Mysko, J.C. Berg, Mechanisms influencing the stability of a nonaqueous phosphor dispersion, *Ind. Eng. Chem. Res.* 32 (1993) 854–858.
- [42] M. Kosmulski, E. Matijevic, Microelectrophoresis of silica in mixed-solvents of low dielectric-constant, *Langmuir* 7 (1991) 2066–2071.
- [43] D.N.L. McGown, G.D. Parfitt, E. Willis, Stability of non-aqueous dispersions. I. the relationship between surface potential and stability in hydrocarbon media, *J. Colloid Sci.* 20 (1965) 650–664.
- [44] I.D. Morrison, Electrical charges in nonaqueous media, *Colloids Surf. A Physicochem. Eng. Asp.* 71 (1993) 1–37.
- [45] J.P. Teas, Graphic analysis of resin solubilities, *J. Paint Technol.* 40 (1968) 19.
- [46] B.A. Miller-Chou, J.L. Koenig, A review of polymer dissolution, *Prog. Polym. Sci.* 28 (2003) 1223–1270.
- [47] F.M. Fowkes, H. Jinnai, M.A. Mostafa, F.W. Anderson, R.J. Moore, Mechanism of electric charging of particles in non-aqueous liquids, *ACS Symp. Ser.* 200 (1982) 307–324.
- [48] M.E. Labib, The origin of the surface-charge on particles suspended in organic liquids, *Colloids Surf. A Physicochem. Eng. Asp.* 29 (1988) 293–304.